4834–4843 *Nucleic Acids Research, 2010, Vol. 38, No. 14* *Published online 12 April 2010*
doi:10.1093/nar/gkq249

NUDT16 is a (deoxy)inosine diphosphatase, and its deficiency induces accumulation of single-strand breaks in nuclear DNA and growth arrest

Teruaki Iyama, Nona Abolhassani, Daisuke Tsuchimoto*, Mari Nonaka and Yusaku Nakabeppu

Division of Neurofunctional Genomics, Department of Immunobiology and Neuroscience, Medical Institute of Bioregulation, Kyushu University, 3-1-1 Maidashi, Higashi-ku, Fukuoka, 812-8582, Japan

Received December 29, 2009; Revised February 26, 2010; Accepted March 24, 2010

ABSTRACT

Nucleotides function in a variety of biological reactions; however, they can undergo various chemical modifications. Such modified nucleotides may be toxic to cells if not eliminated from the nucleotide pools. We performed a screen for modified-nucleotide binding proteins and identified human nucleoside diphosphate linked moiety X-type motif 16 (NUDT16) protein as an inosine triphosphate (ITP)/xanthosine triphosphate (XTP)/GTP-binding protein. Recombinant NUDT16 hydrolyzes purine nucleoside diphosphates to the corresponding nucleoside monophosphates. Among 29 nucleotides examined, the highest k_{cat}/K_m values were for inosine diphosphate (IDP) and deoxyinosine diphosphate (dIDP). Moreover, NUDT16 moderately hydrolyzes (deoxy)inosine triphosphate ([d]ITP). NUDT16 is mostly localized in the nucleus, and especially in the nucleolus. Knockdown of *NUDT16* in HeLa MR cells caused cell cycle arrest in S-phase, reduced cell proliferation, increased accumulation of single-strand breaks in nuclear DNA as well as increased levels of inosine in RNA. We thus concluded that NUDT16 is a (deoxy)inosine diphosphatase that may function mainly in the nucleus to protect cells from deleterious effects of (d)ITP.

INTRODUCTION

Intracellular free nucleotides play essential roles as precursors in the synthesis of DNA and RNA, and as molecules for energy storage, cofactors of metabolic pathways and regulators of signal transduction. Free nucleotides can, however, undergo various chemical modifications by endogenous and exogenous reactive molecules, some of which are inevitably produced in living cells. Chemical modifications may alter the properties of nucleotides, including their interaction with other molecules (1). Some modified deoxynucleotides are known to be incorporated into and to accumulate in newly synthesized DNA during DNA replication. Modified nucleotides, accumulated in either the nucleotide pool or DNA, may inhibit DNA or RNA polymerases during replication or transcription, reduce polymerase fidelity or alter the DNA structure, thus resulting in mutagenesis and carcinogenesis (2,3), cell death and degenerative disorders (4,5) or senescence and aging (6). In addition to DNA metabolism, the other biological functions of canonical nucleotides may also be adversely affected by modified nucleotides. Therefore, because modified nucleotides are constantly generated under physiological conditions, it is crucially important to understand how they are eliminated from cells.

It had been established that cells are equipped with specific enzymes to hydrolyze modified nucleoside triphosphates to the corresponding monophosphates to avoid their deleterious effects (4,7). Deoxyuridine triphosphatase (dUTPase), for example, hydrolyzes dUTP, thus preventing its incorporation into DNA. We have previously demonstrated that MTH1 hydrolyzes oxidized purine nucleoside triphosphates, such as 8-oxo-2′-deoxyguanosine triphosphate (8-oxo-dGTP) or 8-oxoGTP and prevents their incorporation into DNA or RNA (4).

Deamination of purine bases is one of the major chemical modifications that occurs to nucleotides under physiological conditions (8). Deamination of adenine at C6 or guanine at C2 generates hypoxanthine or xanthine, respectively, suggesting that (deoxy)inosine triphosphate ([d]ITP) and (deoxy)xanthosine triphosphate ([d]XTP) can be generated from (d)ATP and (d)GTP,

*To whom correspondence should be addressed. Tel: +81 92 642 6802; Fax: +81 92 642 6804; Email: daisuke@bioreg.kyushu-u.ac.jp

respectively. Moreover, IMP is abundant in cells as a normal intermediate of *de novo* synthesis of purine nucleotides (9), and most cells can generate IDP or ITP from IMP (10). If IDP is converted to dIDP by ribonucleotide reductase, increased dITP levels will result (11). Incorporation of such deaminated purine nucleotides into DNA or RNA causes genomic mutations or synthesis of abnormal proteins because hypoxanthine and xanthine can mis-pair with cytosine or thymine (12,13).

In human and rodents, ITPA, an inosine triphosphatase (ITPase), has been reported to hydrolyze (d)ITP and XTP to the corresponding nucleoside monophosphates and pyrophosphates (14,15). We have previously reported that *Itpa* knockout (KO) mice die before weaning with features of growth retardation and heart failure. In addition, these mice show accumulation of IMP in cellular RNA in various tissues or accumulation of ITP in the nucleotide pool of erythrocytes (16). The heart failure in *Itpa*-KO mice suggests that an accumulation of ITP in the nucleotide pool might impair some functions of adenosine triphosphate (ATP), such as ATP-dependent actomyosin contraction (17). In humans, some variants of *ITPA* are reported to be associated with decreased ITPase activity (18,19). In erythrocytes of ITPA-deficient individuals, it was established that the level of ITP, which is not detected in normal individuals, is increased to a detectable level, as observed in *Itpa*-KO mice. ITPA deficiency in patients with inflammatory bowel disease is, however, likely to be related to azathioprine intolerance, but does not cause any severe phenotype (19,20). To date, it is not known why ITPA deficiency causes a severe phenotype in mouse but not in humans. We, therefore, hypothesized that human cells are equipped with a compensatory mechanism which can efficiently suppress the ITPA deficiency.

In the present study, to identify novel ITP hydrolyzing enzymes or proteins that target ITP, we performed a comprehensive screen of proteins that specifically bind to ITP immobilized on Sepharose beads. We identified human nucleoside diphosphate linked moiety X-type motif 16 (NUDT16) protein (Swiss-Prot accession no., Q96DE0.2).

MATERIALS AND METHODS

Purification and identification of modified nucleotide-binding proteins

Modified nucleotide-binding proteins were purified and identified with pull-down assays as follows. γ-amino-octyl-nucleoside 5′-triphosphate-Sepharose (phosphate-NTP Sepharose) and/or 2′/3′-*O*-(2-aminoethyl-carbamoyl)-nucleoside 5′-triphosphate-Sepharose (ribose-NTP Sepharose) for GTP, ATP, XTP, ITP, 8-oxo-GTP and 2-OH-ATP were purchased from Jena Bioscience (Jena, Germany) and used for pull-down assays. The cell extract of SH-SY5Y cells was prepared by sonication of cells in lysis buffer [1 ml for 5×10^7 cells, 25 mM Tris–HCl pH 7.5, 100 mM NaCl, 10 mM $MgCl_2$, 0.05% Nonidet P-40 (NP-40), 1 mM dithiothreitol (DTT), 1% protease inhibitor cocktail (Nacalai Tesque, Kyoto, Japan)] and clarified by centrifugation, as described previously (21). Protein concentration in the supernatant was measured with a DC-protein assay kit (Bio-Rad, Hercules, CA, USA) using bovine serum albumin (BSA) as a standard. Twenty microliters of each phosphate-NTP Sepharose, ribose-NTP Sepharose, and Sepharose carrier matrix were individually suspended in 1 ml of the supernatant, incubated for 15 min at 4°C, and washed three times with the lysis buffer without protease inhibitor cocktail. Bound proteins in each pulled-down sample were eluted with 40 μl of 2 × SDS sampling buffer (Sigma-Aldrich, St Louis, MO, USA), separated by SDS-PAGE, stained by silver staining with EzStain Silver kit (ATTO Co., Tokyo, Japan), and analyzed by LC-MS/MS, as described previously (21). Collision-induced dissociation spectra were acquired and compared with those in the International Protein Index (IPI version 3.26; European Bioinformatics Institute, Hinxton, UK) using the MASCOT search engine (Matrix Science, Boston, MA, USA). The high-scoring peptide sequences (MASCOT score >45) assigned by MASCOT were manually confirmed by comparison with the corresponding collision-induced dissociation spectra. Finally, we selected as candidate proteins those proteins for which multiple peptides were identified in this analysis.

Nucleotide-hydrolyzing assay with His-NUDT16

Each substrate nucleotide was incubated in reaction buffer (25 mM Tris–HCl pH 7.5, 150 mM KCl, 5 mM $MgCl_2$, 0.01% NP-40, 100 μg/ml BSA, 1 mM DTT) for 10 min at 37°C. Then, an equal volume of reaction buffer containing 100 μM recombinant NUDT16 with a His-tag at the N terminus (His-NUDT16), was mixed with the substrate solution. The mixture was further incubated at 37°C for 0–60 min, and then mixed with ice-cold EDTA to a final concentration of 50 mM to stop the reaction. The reaction products were clarified by centrifugation at 9000*g* for 5 min at 4°C, and then separated on a Wakopak Handy ODS column (Wako, Osaka, Japan) or on a TSK gel DEAE-2SW column (Tohso, Tokyo, Japan) using an HPLC system, at a flow rate of 0.6 ml/min with HPLC buffer 1 (0.1 M potassium phosphate buffer pH 4.0) or at 0.8 ml/min with HPLC buffer 2 (75 mM sodium phosphate buffer pH 6.4, 5% acetonitrile, 0.4 mM EDTA). Nucleotides were quantified by ultraviolet (UV) absorption. Kinetic parameters, k_{cat} and K_m, were calculated by a fit of the velocity data to the Michaelis−Menten equation using the SigmaPlot analysis software version 11 with Enzyme Kinetics Module 1.3 (Systat Software, San Jose, CA, USA).

Free phosphates were quantified colorimetrically with a modified Malachite Green phosphate detection method using Biomol Green reagent (Enzo Life Sciences International, Plymouth Meeting, PA, USA) (22,23). One-hundred microliters of the Biomol Green reagent was added to 50 μl of each reaction mixture, and the mixture was incubated for 30 min at room temperature. The change in absorbance at 620 nm was measured and used to determine free phosphate concentrations by comparison with a standard curve.

siRNA and transfection

All siRNA oligonucleotides used in this study, *NUDT16* siRNA#1 (*Silencer* Select *NUDT16* siRNA; #s43642), *NUDT16* siRNA#2 (*Silencer NUDT16* siRNA; #: 38731), control siRNA#1 (*Silencer* Select Negative Control #1 siRNA, Cat#4390844) and control siRNA#2 (*Silencer* Negative Control #1 siRNA, Cat#AM4635) were purchased from Applied Biosystems (Foster City, CA, USA). HeLa MR cells were transfected with siRNAs by electroporation using a Microporator-Mini (Digital Bio Technology, Seoul, Korea), according to the manufacturer's instructions. In brief, 10^5 cells were suspended in 10 µl of R buffer (provided in the MicroPoration kit) and mixed with 1 µl of one of the siRNAs (50 µM) before electroporation. The transfected cells were suspended in fresh culture medium. After incubation for 24 h, the cells were reseeded in new culture dishes at a density of $1.515 \times 10^3/cm^2$. After an additional incubation, the cells were subjected to further assays.

Immunofluorescence microscopy for NUDT16 and single-stranded DNA

To perform immunofluorescence microscopy for NUDT16 and single-stranded DNA (ssDNA), HeLa MR cells were seeded onto LaB-Tek two-well chamber slides (Thermo Fisher Scientific, Rockford, IL, USA), 24 h after transfection with control siRNA#1 or *NUDT16* siRNA#1. The cells were further cultured for 48 h and fixed with 4% paraformamide in phosphate buffered saline (PBS) containing 0.1% Triton X-100. The fixed cells were treated with anti-NUDT16 or with anti-nucleolin (sc-8031, Santa Cruz Biotechnology, Santa Cruz, CA, USA) in combination with Alexa Fluor 488-conjugated goat anti-rabbit IgG (A-11034, Invitrogen, Carlsbad, CA, USA) or Alexa Fluor 594-conjugated goat anti-mouse IgG (A-11032, Invitrogen). Nuclei were counterstained with 4′-diamino-2-phenylindole (DAPI) (50 ng/ml; Vector Laboratories, Burlingame, CA, USA). Digitized images were separately captured from identical fields using an LSM-510 Meta confocal microscopy system (Carl Zeiss, Oberkochen, Germany).

To detect ssDNA, slides were incubated with a 100 × dilution of anti-ssDNA (#18731, IBL, Takasaki, Japan) in combination with Alexa Fluor 488-conjugated goat anti-rabbit IgG. The anti-ssDNA antibody was raised against fragmented and denatured bovine DNA, and recognizes single stranded regions of DNA with a length of at least six deoxynucleotides length (24,25). Nuclei were counterstained with DAPI. The slide was observed under an Axioskop 2 plus, equipped with AxioCam and AxioVision software (Carl Zeiss). A total of 100 cells were examined for each preparation.

Quantification of deoxyinosine or inosine by LC-MS/MS

The DNA deoxyinosine or RNA inosine levels were determined as follows. The preparation and digestion of nuclear DNA samples were performed according to methods described previously (26), except that 10 mM 2, 2, 6, 6-tetramethylpiperidine-*N*-oxyl (TEMPO, Wako) and 20 µM 2′-deoxycoformycin, an adenosine deaminase inhibitor, kindly provided by the Chemo-Sero-Therapeutic Research Institute (Kumamoto, Japan), were added to all reagents at all stages of manipulation, according to the method described by Taghizadeh *et al.* (27). RNA was prepared using an RNeasy Mini Kit (Qiagen, Valencia, CA, USA) in the presence of 20 mM TEMPO and 20 µM 2′-deoxycoformycin. DNA or RNA samples were digested with Nuclease P1 (Yamasa, Chiba, Japan) and alkaline phosphatase (Sigma-Aldrich) in the presence of 20 mM TEMPO and 20 µM 2′-deoxycoformycin, and digested samples were subjected to LC-MS/MS analysis using the Shimadzu VP-10 HPLC system connected to the API3000 MS/MS system (PE-SCIEX), as described previously (26).

Cell cycle analysis

Flow cytometric analysis of the cell cycle was performed as previously described (28,29). Briefly, 1×10^6 cells were suspended in 1 ml PBS containing 0.2% Triton X for the naked nuclei preparation. Then, the cell suspension was passed through a nylon mesh membrane. Five microliters of RNase A (1 mg/ml) and 50 µl of propidium iodide (PI) (1 mg/ml) were then added to the suspension. DNA content and cell numbers were analyzed with an LSR flow cytometer (Becton Dickinson, San Jose, CA, USA). The data were analyzed with CellQuest and ModFit software (Becton Dickinson).

Karyotype analysis

Fifty-percent confluent cultures of HeLa MR cells were treated with 0.1 µg/ml colcemid (Nacalai Tesque) for 30 min and then harvested. After hypotonic treatment (75 mM KCl), cells were fixed in freshly prepared Carnoy's fixative (methanol:acetic acid; 3:1), and the cell suspension was dropped onto a glass slide, air-dried and immediately stained with freshly prepared Giemsa staining solution (Merck, 25 × diluted in PBS) for 20 min. After rinsing the slide twice in PBS and twice in distilled water, a cover slide was mounted onto the air-dried slide with Permount mounting medium (Thermo Fisher Scientific). The slide was observed under an Axio ImagerA.1 plus equipped with AxioCam and AxioVision software (Carl Zeiss). A total of 30 cells in metaphase were examined for each preparation.

Statistical analysis

All results are expressed as the mean ± SD. Statistical analysis was performed using Stat View 5.0 (SAS Institute, Cary, NC, USA) and each method of statistical analysis is shown in detail in the figure legends. $P < 0.05$ was considered statistically significant.

Supplementary materials and methods

Descriptions of the following materials and procedures are provided in Supplemental Experimental Procedures: free nucleotides, synthetic oligonucleotides, isolation of human *NUDT16* and mouse *Nudt16* cDNAs, construction of

expression plasmids, expression and purification of recombinant His-NUDT16 protein, anti-NUDT16, western blot analysis, cell culture, cell proliferation assay, Hoechst 33342/PI assay, real-time quantitative RT-PCR, and comet assay.

RESULTS

NUDT16 selectively binds to ITP, XTP and GTP

To search for ITP-binding proteins, we purified proteins from whole-cell extracts prepared from SH-SY5Y cells using a pull-down method incorporating various NTP-immobilized Sepharose beads (Figure 1A). The purified proteins were fractionated by SDS-PAGE and visualized by silver staining. The proteins in the gel were digested with trypsin and subjected to LC-MS/MS analysis (see 'Materials and Methods' section). By comparing retrieved proteins with multiple peptide sequences among all samples, we identified peptide fragments derived from NUDT16 only in the samples bound to phosphate/ribose-ITP, phosphate/ribose-XTP and ribose-GTP Sepharose beads, but not in samples bound to any other NTP Sepharose beads (Figure 1B and Supplementary Table S1). Western blot analysis of pull-down samples, prepared independently of the above samples using anti-NUDT16, confirmed the LC-MS/MS results by identifying the same nucleotide-binding 20 kDa NUDT16 protein (Figure 1C).

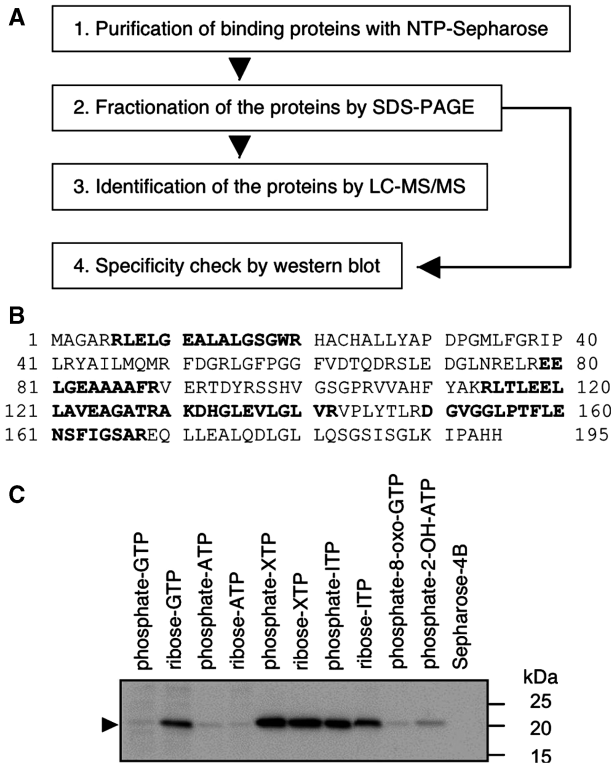

Figure 1. NUDT16 selectively binds to XTP, ITP and GTP. (**A**) Experimental scheme depicting the screen for nucleotide-binding proteins. Proteins in extracts prepared from SH-SY5Y cells were pulled down with NTP-immobilized Sepharose beads and subjected to SDS-PAGE, LC-MS/MS analysis and western blot analysis. (**B**) Amino acid sequence of NUDT16. Peptides detected by LC-MS/MS analysis in the screen are shown in bold (Mascot Ion Score >45). (**C**) Each sample, pulled down from the extract (219 μg total protein), was subjected to western blot analysis using anti-NUDT16 (lower panel). An arrowhead indicates signals for NUDT16.

NUDT16 is a (deoxy)inosine diphosphatase

Because NUDT16 is a member of the nudix family of proteins, including the nucleoside triphosphatase MTH1 (NUDT1), we performed biochemical analysis of nucleotide hydrolyzing activity using recombinant NUDT16 protein. His-NUDT16 was expressed in *Escherichia coli* (*E. coli*) and then purified. Samples from each purification step were subjected to SDS-PAGE and a His-NUDT16 polypeptide of ~23 kDa, (its calculated molecular weight is 23.45 kDa) was purified to near homogeneity after size exclusion column chromatography (Figure 2A).

When several canonical nucleotides were incubated with the purified His-NUDT16 protein, we found that His-NUDT16 effectively hydrolyzed IDP to IMP (Figure 2B, lower). We then determined the optimal conditions for the IDP hydrolysis by His-NUDT16. His-NUDT16 exhibited a temperature-dependent increase in its IDP hydrolyzing activity up to 60°C (Supplementary Figure S1A). IDP hydrolysis by His-NUDT16 gradually increased from pH 6.5 to 8.5 (Supplementary Figure S1B). IDP hydrolysis by His-NUDT16 was completely dependent on the presence of divalent cation, and increased linearly with increasing Mg^{2+} concentration up to 1 mM and then reached a plateau level (Supplementary Figure S1C). Zn^{2+} also increased His-NUDT16 activity in a dose-dependent manner, however, the activity observed in the presence of 10 mM Zn^{2+} was less than one-third of that observed in the presence of 1 mM Mg^{2+}. His-NUDT16 exhibited no IDP hydrolysis in the presence of 5 mM Mn^{2+}, Co^{2+} or Ca^{2+}. KCl, and to a lesser extent NaCl, moderately increased the activity in a dose-dependent manner up to 500 mM (Supplementary Figure S1D). Based on these results and in view of physiological conditions, we performed subsequent analyses of His-NUDT16 activity under the conditions of 25 mM Tris–HCl (pH 7.5), 5 mM Mg^{2+} and 150 mM KCl at 37°C.

To obtain an over view of substrate specificity for NUDT16, we incubated His-NUDT16 with various nucleotides at 10 or 100 μM (Figure 2C). The products were then analyzed and quantified by HPLC. His-NUDT16 hydrolyzed nucleoside triphosphates/diphosphates (NTPs/NDPs) to the corresponding nucleoside monophosphates (NMPs), and had substrate preferences for purine nucleotides. Especially at substrate concentrations of 10 μM, ITP, dITP, XDP, GDP, dGDP, IDP and dIDP were efficiently hydrolyzed. In contrast, His-NUDT16 did not generate any hydrolyzed product from 7-Me-GDP, ATP, CTP, UTP, 2-OH-ATP, dATP, dCTP, dUTP, TTP nor 2-OH-dATP, even at 100 μM. Because these substrates were not hydrolyzed, they are not represented in Figure 2C.

His-NUDT16 produced IMP from both ITP and IDP (Supplementary Figure S2 upper). To confirm the

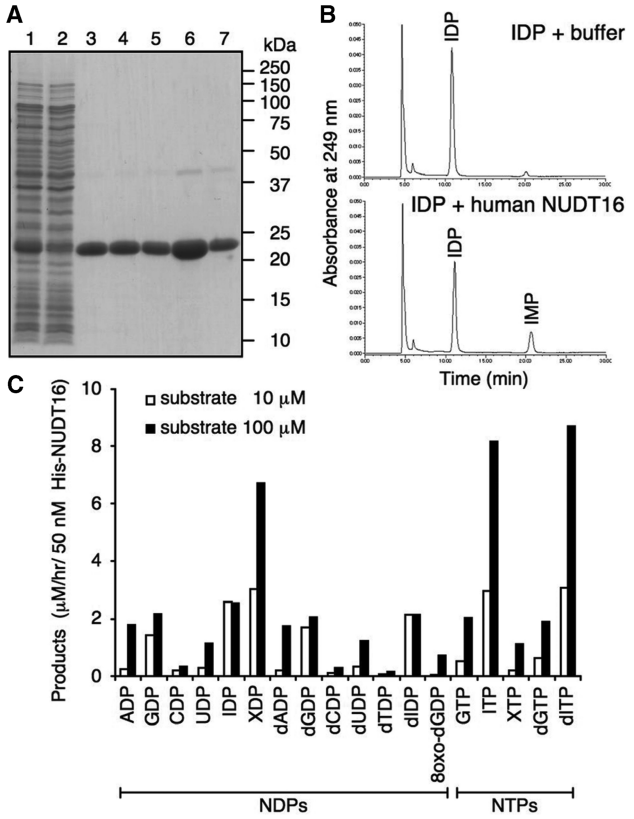

Figure 2. His-NUDT16 hydrolyzes (d)IDP in preference to other nucleotides. (**A**) Samples from the purification of recombinant His-NUDT16 were subjected to SDS-PAGE and GelCode Blue Staining. Lane 1, supernatant of *E. coli* extract; lane 2, flow-through fraction from the His-tag purification; lane 3, eluate from His-tag purification; lane 4, fraction recovered by ammonium sulfate precipitation; lane 5, sample after dialysis; lane 6, eluate from cation exchange chromatography; lane 7, fraction recovered from gel filtration chromatography. (**B**) IDP (200 μM) was incubated with 400 nM His-NUDT16 for 1 h at 37°C. Reaction products were analyzed by HPLC (lower panel), and were compared with substrate IDP incubated without His-NUDT16 (upper panel). HPLC chromatograms of both samples obtained by absorbance at 249 nm are shown. (**C**) Nucleoside di- or triphosphates (10 or 100 μM) were incubated with 50 nM His-NUDT16 for 1 h at 37°C. The reaction products were analyzed by HPLC. The graph shows the concentration of each nucleoside monophosphate product.

generation of free phosphates (Pi) in these reactions, we analyzed the products using the Malachite Green phosphate detection method to distinguish Pi from pyrophosphates (PPi). Hydrolysis of IDP by His-NUDT16 generated almost the same amounts of IMP and Pi; however, hydrolysis of ITP by His-NUDT16 generated IMP but not Pi (Supplementary Figure S2 lower). These results indicate that NUDT16 hydrolyzes IDP to IMP and Pi, while ITP is hydrolyzed to IMP and possibly PPi.

Because His-NUDT16 efficiently hydrolyzed ITP, dITP, XDP, GDP, dGDP, IDP and dIDP, we performed a detailed analysis of the hydrolysis kinetics for these substrates (Table 1). Fitting Michaelis–Menten type kinetics to the initial rates of reaction revealed a positive correlation for each substrate. Among the substrates, the k_{cat}/K_m values for IDP and dIDP were 251×10^3 and $183 \times 10^3\ s^{-1}\ M^{-1}$, respectively. These were at least seven times higher than the k_{cat}/K_m value for GDP ($26.2 \times 10^3\ s^{-1}\ M^{-1}$), which was the third highest among the substrates analyzed. IDP and dIDP were, therefore, identified as the best substrates for His-NUDT16.

Table 1. Kinetic parameters of His-NUDT16

Substrate	K_m μM	k_{cat} min^{-1}	k_{cat}/K_m $10^3\ s^{-1}\ M^{-1}$	Goodness-of-curve fit R^2
IDP	0.062	0.931	251	0.973
dIDP	0.088	0.966	183	0.990
GDP	0.330	0.518	26.1	0.987
dGDP	0.319	0.492	25.7	0.988
XDP	15.7	2.60	2.76	0.978
ITP	22.1	3.06	2.31	0.980
dITP	24.1	3.20	2.21	0.999

We also expressed mouse His-tagged NUDT16 protein (His-mNUDT16) in *E. coli* and analyzed dITP hydrolyzing activity using extracts prepared from *E. coli* cells with or without expression of His-mNUDT16. *E. coli* extract without His-mNUDT16 generated dIDP and dIMP from dITP. In contrast, *E. coli* extract with His-mNUDT16 generated only dIMP from dITP (Supplementary Figure S3). Thus, we concluded that mouse NUDT16 also hydrolyzes dIDP to dIMP.

Expression of NUDT16 in human cell lines and tissues

We determined the levels of *NUDT16* mRNA in 21 human tissues by real-time quantitative RT-PCR (Supplementary Figure S4). *NUDT16* mRNA was detected in all tissues examined and the highest expression was observed in lung and kidney. Next, we examined levels of *NUDT16* mRNA and protein in HeLa MR cells with or without (si)RNA silencing. Real-time quantitative RT-PCR revealed that *NUDT16* mRNA levels in HeLa MR cells were equivalent to those in heart and mammary gland. The introduction of *NUDT16* siRNA#1 significantly reduced the mRNA level to 17% of the control after 3 days (Figure 3A). Western blot analysis with anti-NUDT16 revealed a significantly reduced expression of a 20 kDa protein in HeLa MR cells, 2 and 4 days after the introduction of *NUDT16* siRNA#1 (Figure 3B). Other bands were consistently and uniformly detected in samples from cells treated with control siRNA#1 and *NUDT16* siRNA#1. The expression of the 20 kDa band partially recovered 7 days after the treatment, thus demonstrating that the 20 kDa protein is the endogenous NUDT16 protein of HeLa MR cells.

Next, we examined subcellular localization of NUDT16 protein in HeLa MR cells by immunofluorescence confocal laser scanning microscopy with anti-NUDT16 and anti-nucleolin, a nucleolar marker (Figure 3C). NUDT16 immunoreactivity was mostly detected in the DAPI-positive nuclei and partially detected in the cytoplasm (Figure 3C-a,b,d). The signal for NUDT16 was not uniformly localized in nuclei, but was intensely localized in a few small regions. The intense NUDT16 signals were mostly colocalized with the intense nucleolin signals where DAPI signals were faint (Figure 3C-d–f).

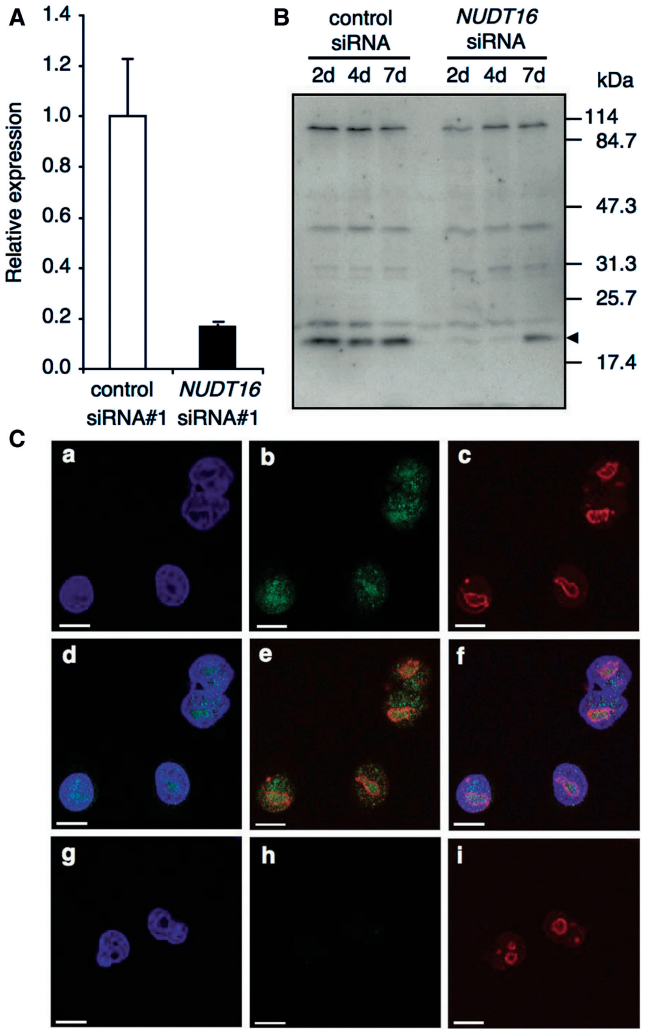

Figure 3. NUDT16 is mainly localized in nuclei, and especially in nucleoli. (**A**) Relative mRNA level after transfection of *NUDT16* siRNA. Three days after transfection with siRNAs, cells were harvested. The *NUDT16* mRNA level relative to that of the control was determined by real time quantitative RT-PCR and is shown as the mean ± SD of triplicate experiments. (**B**) Cells were transfected with siRNAs and harvested 2, 4, and 7 days after transfection. Cell extracts (10 μg total protein) were subjected to western blot analysis with anti-NUDT16. An arrowhead indicates signals for NUDT16. (**C**) Intracellular localization of NUDT16. HeLa MR cells were transfected with control siRNA#1 (a–f) or with *NUDT16* siRNA#1 (g–i). The cells were subjected to immunofluorescence microscopy with anti-NUDT16 (green, b and h) and anti-nucleolin (red, c and i). Nuclei were stained with DAPI (blue, a and g). Merged signals are shown in panel d (blue and green), e (green and red) and f (blue, green and red). Bars indicate 10 μm.

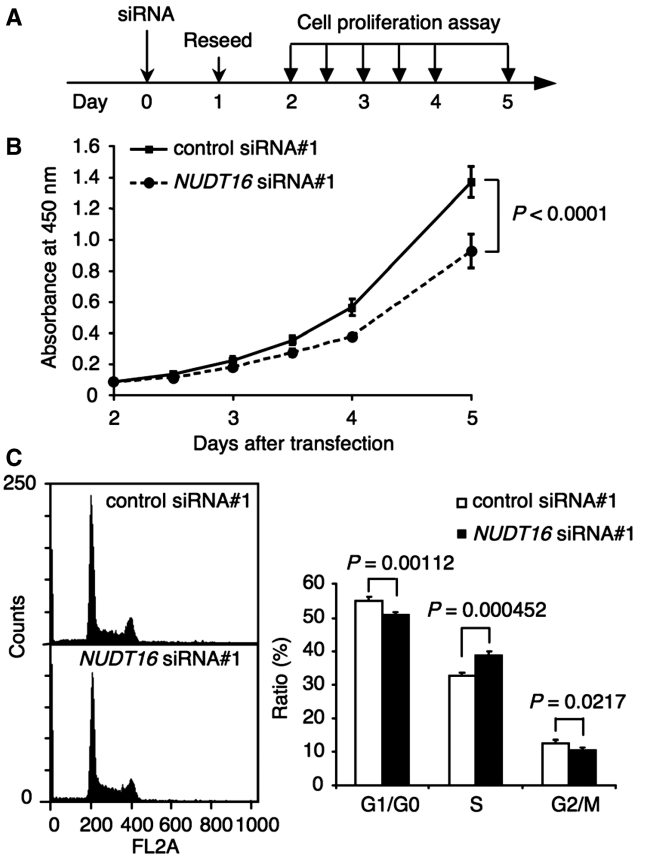

Figure 4. Knockdown of *NUDT16* suppresses proliferation of HeLa MR cells. (**A**) Experimental schedule. HeLa MR cells were transfected with siRNAs on Day 0. The transfected cells were then further incubated for 24 h before replating at a density of $1.5 \times 10^3/cm^2$. After an additional incubation, the cells were subjected to further analysis. (**B**) Cell proliferation assay. The cells in (A) were analyzed for cell proliferation. The graph shows the mean ± SD of results from three independent siRNA transfections. Two-way repeated measures ANOVA, $P < 0.0001$. (**C**) HeLa MR cells treated with *NUDT16* siRNA#1 show slightly abnormal progression of the cell cycle. Three days after siRNA transfection with *NUDT16* siRNA#1 or with control siRNA#1, cells were subjected to flow cytometry. Left panels indicate representative histograms of DNA contents in isolated nuclei from these cells. Data are mean ± SD of results from three independent siRNA transfections and were analyzed using Student's *t*-test.

Furthermore, most of the NUDT16 signals disappeared in cells treated with *NUDT16* siRNA#1 (Figure 3C-h). We thus concluded that NUDT16 protein is mostly localized in nucleoli.

Knockdown of NUDT16 expression suppresses proliferation of HeLa MR cells

To elucidate the biological functions of NUDT16, we examined the effects of *NUDT16* knockdown in HeLa MR cells. Twenty-four hours after the introduction of siRNA, the cells were reseeded. We then compared cell proliferation rates between cells treated with control siRNA#1 and those treated with *NUDT16* siRNA#1 (Figure 4A). *NUDT16* siRNA#1 significantly suppressed cell proliferation compared with the control siRNA (Figure 4B). Introduction of *NUDT16* siRNA#2, which has a different target sequence for *NUDT16*, also similarly suppressed the proliferation of HeLa MR cells, confirming the effect of *NUDT16* knockdown (Supplementary Figure S5A and B). Next, we performed a flow cytometric analysis of DNA content of HeLa MR cells after *NUDT16* knockdown. Cell cycle analysis revealed significantly increased S-phase and decreased G1 phase populations after introduction of *NUDT16* siRNA#1 (Figure 4C). Moreover, Hoechst 33342/PI

staining of the cells revealed that introduction of *NUDT16* siRNA#1 caused no obvious increase in the dead cell fraction (PI positive) in comparison to control siRNA#1 (Supplementary Figure S6). We observed no subG1 fraction, indicating that *NUDT16* knockdown did not induce cell death in our experimental conditions (Figure 4C).

Accumulation of inosine nucleotides in RNA and of single strand breaks in DNA after knockdown of NUDT16 expression

The localization of NUDT16 in nuclei strongly suggested that NUDT16 contributes to sanitization of the nuclear nucleotide pool, which supplies precursors for the synthesis of RNA and DNA. We, therefore, measured inosine in cellular RNA and deoxyinosine in nuclear DNA in HeLa MR cells after *NUDT16* knockdown by siRNA. The inosine level in RNA was significantly increased in cells treated with *NUDT16* siRNA#1 (36.1 ± 1.35 inosine residues per 10^6 guanosine residues) compared with cells treated with control siRNA#1 (31.9 ± 1.05 inosine residues per 10^6 guanosine residues) ($P = 0.0125$) (Figure 5A right). However, there was no significant difference in the deoxyinosine level in DNA between the two conditions (Figure 5A left). These results suggested that ITP or dITP levels are increased after *NUDT16* knockdown, and that their incorporation into RNA or DNA may be similarly increased; however, deoxyinosine incorporated into newly synthesized DNA might be quickly eliminated by DNA repair enzymes. DNA repair processes often form ssDNA regions as repair intermediates (30–32). Therefore, we examined ssDNA accumulation in nuclear DNA of HeLa MR cells by immunofluorescence detection using an anti-ssDNA antibody after siRNA treatment. The anti-ssDNA antibody was raised against fragmented bovine DNA, and recognizes ssDNA generated by double- or single-strand DNA breaks (33). Following treatment with *NUDT16* siRNA, the percentage of ssDNA-positive HeLa MR cells (13.9%) was 5.3 times higher than that treated with control siRNA ($P = 0.000252$) (Figure 5B). ssDNA regions can be generated by either single- or double-strand breaks in DNA. In the comet assay, HeLa

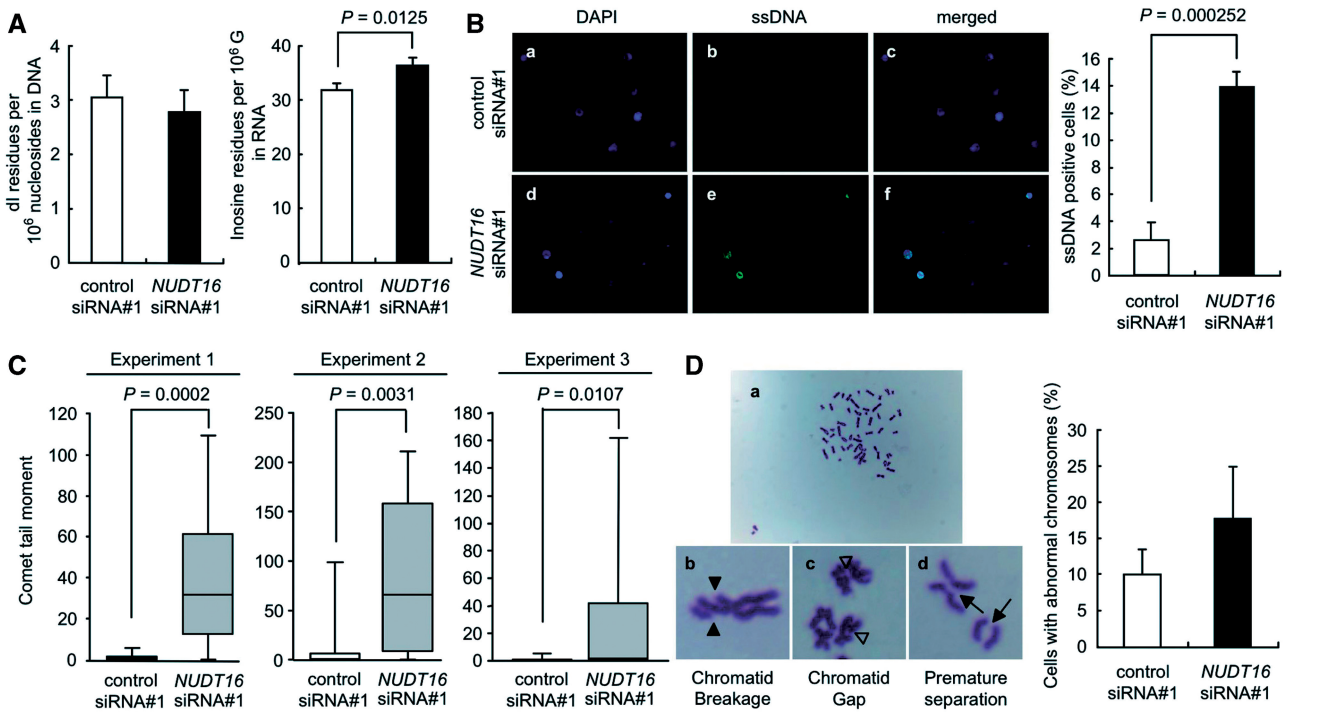

Figure 5. Knockdown of *NUDT16* in HeLa MR cells increases the number of inosine residues in RNA and the level of single strand breaks in nuclear DNA. HeLa MR cells were independently transfected with siRNAs three times. Three days after transfection, cells were subjected to the following analysis. (**A**) Quantification of inosine or deoxyinosine by LC-MS/MS. HeLa MR cells were harvested to determine the levels of inosine and deoxyinosine [dI]. The numbers of deoxyinosine residues [dI] per 10^6 nucleosides in DNA or inosine residues per 10^6 guanosine [G] in RNA from three independent transfections are shown. Student's *t*-test, $P = 0.0125$ (RNA). (**B**) Knockdown of *NUDT16* induces the accumulation of ssDNA in nuclei of HeLa MR cells. HeLa MR cells transfected with control siRNA#1 (a–c) or with *NUDT16* siRNA#1 (d–f) were subjected to immunofluorescence microscopy with anti-ssDNA (green, b and e). Nuclei were stained with DAPI (blue, a and d). Merged signals are shown in c and f (blue and green). Percentages of ssDNA-positive nuclei among DAPI-positive nuclei are shown in the bar graph. Data are mean ± SD of three independent siRNA transfections. Student's *t*-test, $P = 0.000252$. (**C**) Comet assay under alkaline conditions. Tail moments of at least 15 cells were calculated for each group and box-and-whisker plots are shown for three independent assays. Mann–Whitney U-test, $P < 0.05$. (**D**) Chromosomal abnormality. Transfected cells were prepared as in (B). Mitotic cells with chromosomal abnormalities (a) were defined as cells with chromatid breakage (b; solid arrowheads), chromatid gap (c; open arrowheads) and/or premature separation (d; arrows). These cells were counted and percentages of cells with chromosomal abnormalities among thirty mitotic cells are shown in the bar graph. Chromatid breakage, chromatid gap, and premature separation in control cells were 8%, 2% and 0%, respectively, and in *NUDT16* knockdown cells were12%, 4% and 1%, respectively. Data are mean ± SD from three independent siRNA transfections.

MR cells transfected with *NUDT16* siRNA showed a significantly increased tail moment under alkaline conditions in three independent experiments ($P < 0.05$, Mann–Whitney U-test), but not under neutral conditions (Figure 5C and Supplementary Figure S7). Cells exposed to hydrogen peroxide, which is known to cause double-strand breaks, exhibited a significantly increased tail moment, even under neutral conditions; therefore we concluded that knockdown of *NUDT16* caused accumulation of single-strand breaks in nuclear DNA. Next, chromosome abnormalities including chromatid breakage, chromatid gap, and/or premature separation were examined in mitotic cells. The percentage of the cells with abnormal chromosomes in HeLa MR cells treated with *NUDT16* siRNA was 1.8 times higher than that in cells treated with control siRNA, although the difference was not significant ($P = 0.115$) (Figure 5D).

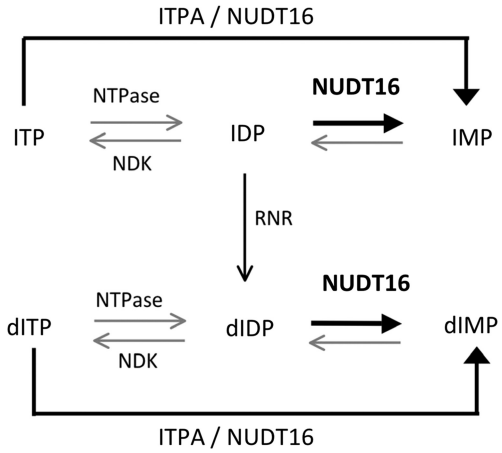

Figure 6. Model of biological roles of NUDT16. NUDT16 eliminates (d)IDP and (d)ITP from the nucleotide pools in cooperation with ITPA. NDK; nucleoside diphosphate kinases, RNR; ribonucleotide reductase.

DISCUSSION

In the present study, we reported two major findings; first, NUDT16 hydrolyzes (d)IDP/(d)ITP and second, NUDT16 deficiency induces accumulation of single strand breaks in nuclear DNA and growth arrest in human cells.

Previously, Ghosh *et al.* (34) reported that NUDT16 recognizes the 5′-cap structure of U8 small nucleolar RNA (snoRNA) and weakly hydrolyzes it to produce non-capped-snoRNA with guanosine 5′-monophosphate at its 5′-terminus and an excised cap. First guanosine residue of U8 snoRNA itself is linked to the triphosphate following the 5′-cap, and thus mimicking a GTP structure. GTP was shown to be weakly hydrolyzed by NUDT16 in the present study. Therefore, both 5′-capped U8 snoRNA and GTP can be converted by NUDT16 to guanosine 5′-monophosphate (GMP) at the 5′-terminal end of snoRNA and to free GMP, respectively. Thus, it is likely that hydrolysis of GTP and decapping of U8 snoRNA are essentially the same enzyme reaction of NUDT16. We also showed that in a human cell line, NUDT16 is localized in nuclei, mainly nucleoli. Similarly, Ghosh *et al.* (34) have reported that X29 protein, the *Xenopus* homolog of NUDT16, is primarily a nucleolar protein in *Xenopus* cells *in vitro*.

As shown in Figure 6, NUDT16 efficiently hydrolyzes (d)IDP, and hydrolyzes (d)ITP to a lesser extent. (d)ITP and (d)IDP can be generated by deamination of adenine nucleotides or phosphorylation of (d)IMP (35). ITPA, which is relatively abundant in the cytoplasm and which is encoded by *ITPA*, is known to hydrolyze (d)ITP to (d)IMP and pyrophosphate (14,15). The study of NUDT16 reaction kinetics revealed that NUDT16 has a lower hydrolysis rate but a higher affinity for (d)ITP compared with ITPA (for ITP; NUDT16, k_{cat} 3.2 min^{-1}, K_m 22.1 μM; ITPA, k_{cat} 34 800 min^{-1}, K_m 510 μM) (15). NUDT16, therefore, might be an important enzyme for the elimination of (deoxy)inosine nucleotides from nuclei, especially at low concentrations. Because NUDT16 is localized mainly in nucleoli, NUDT16 may prevent the incorporation of inosine nucleotides into ribosomal RNA (rRNA) during transcription. An increase in the RNA inosine level, observed after the knockdown of *NUDT16* supports this hypothesis. NUDT16, but not ITPA, has a strong hydrolysis activity for (d)IDP. In the pathway converting abundant cellular IMP to ITP by phosphorylation (10), IDP is an important intermediate. In addition, IDP is expected to be converted to dIDP by ribonucleotide reductase (36), and dIDP can be phosphorylated, thereby resulting in increased levels of dITP (11).

8-oxo-dGTP is known to be incorporated into genomic DNA and to induce mutation in both mammalian and bacterial cells (3). Human NUDT5, which hydrolyzes 8-oxo-dGDP, was reported to decrease spontaneous mutation in *E. coli mutT*$^-$ cells deficient in 8-oxo-dGTP hydrolyzing activity (37). Taken together with our findings on NUDT16, these results support the importance of the elimination of modified (deoxy)nucleoside diphosphates from the nucleotide pools.

In the present study, we observed the deoxyinosine levels in nuclear DNA within the normal ranges previously observed by Taghizadeh *et al.* (27) even after knockdown of *NUDT16*. However, knockdown of *NUDT16* expression increased the fraction of ssDNA-positive cells. We assume that the dITP level in the nuclear nucleotide pool must increase after *NUDT16* knockdown, thus resulting in increased incorporation of deoxyinosine into newly synthesized DNA. The deoxyinosine in DNA is immediately removed by the DNA repair process, resulting in an accumulation of ssDNA. Bradshaw and Kuzminov (38) described the incorporation of dITP/dXTP into the genomic DNA of *rdgB*$^-$ *E. coli* cells, which lack bacterial ITPase. In *E. coli* cells, DNA containing deoxyinosine can be excised by Endo V-initiated nucleotide excision repair, thus resulting in DNA strand breakage (32). Both Endo V and another enzyme, alkyl-adenine-DNA glycosylase (AAG, MAG, ANPG, MPG) were reported as candidates for hypoxanthine specific DNA repair enzymes in

mammalian cells (39–41). It is well known that increased accumulation of ssDNA triggers the DNA damage response, to induce delay in S-phase, and then cell cycle arrest (42). We, therefore, assume that the DNA damage response, to the accumulation of ssDNA, suppresses cell cycle progression, thus increasing the S-phase population and resulting in a decreased proliferation rate. On the other hand, knockdown of NUDT16 expression induced a 13.3% increase in RNA inosine levels. RNA editing by adenosine deaminases is a well-known system of post-transcriptional regulation and the major source of inosine in RNA; therefore, more inosine residues are present in RNA compared with deoxyinosine residues in DNA (43,44). Inosine, produced in RNA by such a regulated system, is thought to cause important modifications to the functions of non-coding RNA, or to alter amino acid sequence encoded by mRNA (45,46). In other words, unregulated incorporation of inosine during RNA transcription might impair RNA functions. In the present study, we demonstrated that NUDT16 contributes to the suppression of such inosine incorporation into RNA. Although the increased level of inosine in RNA under NUDT16 deficiency was statistically significant and the net increase was much higher than the basal level of deoxyinosine in DNA (4.3 inosine/10^6 G versus 0.63 deoxyinosine/10^6 dG), the higher basal level of inosine in RNA (32 inosine/10^6 G), which is likely to be generated by RNA-editing (45,46), made the difference appear small.

We previously reported that *Itpa*$^{-/-}$ mice showed growth retardation and heart failure and did not survive beyond 2 weeks after birth (16). Following this report, we found that primary mouse embryonic fibroblasts (MEFs) prepared from *Itpa*$^{-/-}$ mice showed a significantly prolonged doubling time and chromosomal abnormalities, accompanied by increased ssDNA and deoxyinosine residues in nuclear DNA (47). However, once *Itpa*$^{-/-}$ MEFs were spontaneously immortalized, the immortalized *Itpa*$^{-/-}$ MEFs had neither of these phenotypes. Furthermore, immortalized *Itpa*$^{-/-}$ MEFs exhibited significantly increased levels of *Nudt16* mRNA and protein. siRNA-mediated knockdown of *Nudt16* in immortalized *Itpa*$^{-/-}$ MEFs significantly increased deoxyinosine levels in nuclear DNA, and thus reproduced the ITPA-deficient phenotype. We, therefore, concluded that mouse NUDT16 functions as a backup enzyme for the ITPA deficiency by eliminating (d)IDP, and to a lesser extent (d)ITP from the nucleotide pools in MEFs. In wild-type MEFs, knockdown of *Nudt16* did not result in such phenotypes, indicating that mouse ITPA can compensate for the deficiency of NUDT16 in MEFs. In contrast, our present data suggested that human ITPA itself cannot completely compensate for the deficiency of NUDT16 in HeLa MR cells, although double deficiency of ITPA and NUDT16 would cause more severe phenotypes. Human individuals with ITPA deficiency show no obvious phenotypes. Thus, ITPA deficiency causes quite different effects in mouse and human. Comparing the expression level or enzyme activity of NUDT16 between mouse and human might explain why human cells have a significant tolerance to ITPA deficiency. In the present study, partial reduction of *NUDT16* expression in HeLa MR cells was sufficient to cause growth suppression and accumulation of single-strand breaks in nuclear DNA. Therefore, defective NUDT16 might lead to genome-instability syndromes in human individuals.

SUPPLEMENTARY DATA

Supplementary Data are available at NAR Online.

ACKNOWLEDGEMENTS

We thank Drs M. Matsumoto and K. Oyamada, from the Division of Cell Biology of the Medical Institute of Bioregulation, for helpful discussions. We thank M. Oda, E. Koba and M. Ohtsu, from the Laboratory for Technical Support of the Medical Institute of Bioregulation, and N. Adachi and K. Asakawa for their technical assistance.

FUNDING

The Ministry of Education, Culture, Sports, Science and Technology of Japan (20013034 to Y.N., 21117512 to D.T.); Japan Society for the Promotion of Science (19390114 to D.T., 08J03650 to T.I.); Kyushu University Global COE program (to Y.N.). Funding for open access charge: The Ministry of Education, Culture, Sports, Science and Technology of Japan (21117512 to D.T.).

Conflict of interest statement. None declared.

REFERENCES

1. Friedberg,E.C., Walker,G.C., Siede,W., Wood,R.D., Schultz,R.A. and Ellenberger,T. (2005) *DNA Repair And Mutagenesis*, 2nd edn. ASM Press, Washington.
2. Nakabeppu,Y., Sakumi,K., Sakamoto,K., Tsuchimoto,D., Tsuzuki,T. and Nakatsu,Y. (2006) Mutagenesis and carcinogenesis caused by the oxidation of nucleic acids. *Biol. Chem.*, **387**, 373–379.
3. Tsuzuki,T., Nakatsu,Y. and Nakabeppu,Y. (2007) Significance of error-avoiding mechanisms for oxidative DNA damage in carcinogenesis. *Cancer Sci.*, **98**, 465–470.
4. Nakabeppu,Y., Kajitani,K., Sakamoto,K., Yamaguchi,H. and Tsuchimoto,D. (2006) MTH1, an oxidized purine nucleoside triphosphatase, prevents the cytotoxicity and neurotoxicity of oxidized purine nucleotides. *DNA Repair*, **5**, 761–772.
5. Nakabeppu,Y., Tsuchimoto,D., Yamaguchi,H. and Sakumi,K. (2007) Oxidative damage in nucleic acids and Parkinson's disease. *J. Neurosci. Res.*, **85**, 919–934.
6. Rai,P., Onder,T.T., Young,J.J., McFaline,J.L., Pang,B., Dedon,P.C. and Weinberg,R.A. (2009) Continuous elimination of oxidized nucleotides is necessary to prevent rapid onset of cellular senescence. *Proc. Natl Acad. Sci. USA*, **106**, 169–174.
7. el-Hajj,H.H., Zhang,H. and Weiss,B. (1988) Lethality of a *dut* (deoxyuridine triphosphatase) mutation in *Escherichia coli*. *J. Bacteriol.*, **170**, 1069–1075.
8. Nguyen,T., Brunson,D., Crespi,C.L., Penman,B.W., Wishnok,J.S. and Tannenbaum,S.R. (1992) DNA damage and mutation in human cells exposed to nitric oxide in vitro. *Proc. Natl Acad. Sci. USA*, **89**, 3030–3034.
9. Traut,T.W. (1994) Physiological concentrations of purines and pyrimidines. *Mol. Cell. Biochem.*, **140**, 1–22.
10. Vanderheiden,B.S. (1979) Inosine di- and triphosphate synthesis in erythrocytes and cell extracts. *J. Cell. Physiol.*, **99**, 287–301.

11. Myrnes,B., Guddal,P.H. and Krokan,H. (1982) Metabolism of dITP in HeLa cell extracts, incorporation into DNA by isolated nuclei and release of hypoxanthine from DNA by a hypoxanthine-DNA glycosylase activity. *Nucleic Acids Res.*, **10**, 3693–3701.
12. Schouten,K.A. and Weiss,B. (1999) Endonuclease V protects *Escherichia coli* against specific mutations caused by nitrous acid. *Mutat. Res.*, **435**, 245–254.
13. Yasui,M., Suenaga,E., Koyama,N., Masutani,C., Hanaoka,F., Gruz,P., Shibutani,S., Nohmi,T., Hayashi,M. and Honma,M. (2008) Miscoding properties of 2′-deoxyinosine, a nitric oxide-derived DNA Adduct, during translesion synthesis catalyzed by human DNA polymerases. *J. Mol. Biol.*, **377**, 1015–1023.
14. Behmanesh,M., Sakumi,K., Tsuchimoto,D., Torisu,K., Ohnishi-Honda,Y., Rancourt,D.E. and Nakabeppu,Y. (2005) Characterization of the structure and expression of mouse *Itpa* gene and its related sequences in the mouse genome. *DNA Res.*, **12**, 39–51.
15. Lin,S., McLennan,A.G., Ying,K., Wang,Z., Gu,S., Jin,H., Wu,C., Liu,W., Yuan,Y., Tang,R. *et al.* (2001) Cloning, expression, and characterization of a human inosine triphosphate pyrophosphatase encoded by the *ITPA* gene. *J. Biol. Chem.*, **276**, 18695–18701.
16. Behmanesh,M., Sakumi,K., Abolhassani,N., Toyokuni,S., Oka,S., Ohnishi,Y.N., Tsuchimoto,D. and Nakabeppu,Y. (2009) ITPase-deficient mice show growth retardation and die before weaning. *Cell Death Differ.*, **16**, 1315–1322.
17. Burton,K., White,H. and Sleep,J. (2005) Kinetics of muscle contraction and actomyosin NTP hydrolysis from rabbit using a series of metal-nucleotide substrates. *J. Physiol.*, **563**, 689–711.
18. Maeda,T., Sumi,S., Ueta,A., Ohkubo,Y., Ito,T., Marinaki,A.M., Kurono,Y., Hasegawa,S. and Togari,H. (2005) Genetic basis of inosine triphosphate pyrophosphohydrolase deficiency in the Japanese population. *Mol. Genet. Metab.*, **85**, 271–279.
19. Sumi,S., Marinaki,A.M., Arenas,M., Fairbanks,L., Shobowale-Bakre,M., Rees,D.C., Thein,S.L., Ansari,A., Sanderson,J., De Abreu,R.A. *et al.* (2002) Genetic basis of inosine triphosphate pyrophosphohydrolase deficiency. *Hum. Genet.*, **111**, 360–367.
20. Marinaki,A.M., Duley,J.A., Arenas,M., Ansari,A., Sumi,S., Lewis,C.M., Shobowale-Bakre,M., Fairbanks,L.D. and Sanderson,J. (2004) Mutation in the *ITPA* gene predicts intolerance to azathioprine. *Nucleosides Nucleotides Nucleic Acids*, **23**, 1393–1397.
21. Nonaka,M., Tsuchimoto,D., Sakumi,K. and Nakabeppu,Y. (2009) Mouse RS21-C6 is a mammalian 2′-deoxycytidine 5′-triphosphate pyrophosphohydrolase that prefers 5-iodocytosine. *FEBS J.*, **276**, 1654–1666.
22. Klaus,S.M., Wegkamp,A., Sybesma,W., Hugenholtz,J., Gregory,J.F.III. and Hanson,A.D. (2005) A nudix enzyme removes pyrophosphate from dihydroneopterin triphosphate in the folate synthesis pathway of bacteria and plants. *J. Biol. Chem.*, **280**, 5274–5280.
23. Xu,W., Shen,J., Dunn,C.A., Desai,S. and Bessman,M.J. (2001) The Nudix hydrolases of *Deinococcus radiodurans*. *Mol. Microbiol.*, **39**, 286–290.
24. Oka,S., Ohno,M., Tsuchimoto,D., Sakumi,K., Furuichi,M. and Nakabeppu,Y. (2008) Two distinct pathways of cell death triggered by oxidative damage to nuclear and mitochondrial DNAs. *EMBO J.*, **27**, 421–432.
25. Kawarada,Y., Miura,N. and Sugiyama,T. (1998) Antibody against single-stranded DNA useful for detecting apoptotic cells recognizes hexadeoxynucleotides with various base sequences. *J. Biochem.*, **123**, 492–498.
26. Tsuruya,K., Furuichi,M., Tominaga,Y., Shinozaki,M., Tokumoto,M., Yoshimitsu,T., Fukuda,K., Kanai,H., Hirakata,H., Iida,M. *et al.* (2003) Accumulation of 8-oxoguanine in the cellular DNA and the alteration of the OGG1 expression during ischemia-reperfusion injury in the rat kidney. *DNA Repair*, **2**, 211–229.
27. Taghizadeh,K., McFaline,J.L., Pang,B., Sullivan,M., Dong,M., Plummer,E. and Dedon,P.C. (2008) Quantification of DNA damage products resulting from deamination, oxidation and reaction with products of lipid peroxidation by liquid chromatography isotope dilution tandem mass spectrometry. *Nat. Protoc.*, **3**, 1287–1298.
28. Yamazaki,K., Guo,L., Sugahara,K., Zhang,C., Enzan,H., Nakabeppu,Y., Kitajima,S. and Aso,T. (2002) Identification and biochemical characterization of a novel transcription elongation factor, Elongin A3. *J. Biol. Chem.*, **277**, 26444–26451.
29. Ide,Y., Tsuchimoto,D., Tominaga,Y., Nakashima,M., Watanabe,T., Sakumi,K., Ohno,M. and Nakabeppu,Y. (2004) Growth retardation and dyslymphopoiesis accompanied by G2/M arrest in APEX2-null mice. *Blood*, **104**, 4097–4103.
30. Hegde,M.L., Hazra,T.K. and Mitra,S. (2008) Early steps in the DNA base excision/single-strand interruption repair pathway in mammalian cells. *Cell Res.*, **18**, 27–47.
31. Demple,B. and DeMott,M.S. (2002) Dynamics and diversions in base excision DNA repair of oxidized abasic lesions. *Oncogene*, **21**, 8926–8934.
32. Weiss,B. (2008) Removal of deoxyinosine from the *Escherichia coli* chromosome as studied by oligonucleotide transformation. *DNA Repair*, **7**, 205–212.
33. Naruse,I., Keino,H. and Kawarada,Y. (1994) Antibody against single-stranded DNA detects both programmed cell death and drug-induced apoptosis. *Histochemistry*, **101**, 73–78.
34. Ghosh,T., Peterson,B., Tomasevic,N. and Peculis,B.A. (2004) *Xenopus* U8 snoRNA binding protein is a conserved nuclear decapping enzyme. *Mol. Cell*, **13**, 817–828.
35. Shenoy,T.S. and Clifford,A.J. (1975) Adenine nucleotide metabolism in relation to purine enzymes in liver, erythrocytes and cultured fibroblasts. *Biochim. Biophys. Acta*, **411**, 133–143.
36. Burgis,N.E. and Cunningham,R.P. (2007) Substrate specificity of RdgB protein, a deoxyribonucleoside triphosphate pyrophosphohydrolase. *J. Biol. Chem.*, **282**, 3531–3538.
37. Ishibashi,T., Hayakawa,H. and Sekiguchi,M. (2003) A novel mechanism for preventing mutations caused by oxidation of guanine nucleotides. *EMBO Rep.*, **4**, 479–483.
38. Bradshaw,J.S. and Kuzminov,A. (2003) RdgB acts to avoid chromosome fragmentation in *Escherichia coli*. *Mol. Microbiol.*, **48**, 1711–1725.
39. Moe,A., Ringvoll,J., Nordstrand,L.M., Eide,L., Bjoras,M., Seeberg,E., Rognes,T. and Klungland,A. (2003) Incision at hypoxanthine residues in DNA by a mammalian homologue of the *Escherichia coli* antimutator enzyme endonuclease V. *Nucleic Acids Res.*, **31**, 3893–3900.
40. Lee,C.Y., Delaney,J.C., Kartalou,M., Lingaraju,G.M., Maor-Shoshani,A., Essigmann,J.M. and Samson,L.D. (2009) Recognition and processing of a new repertoire of DNA substrates by human 3-methyladenine DNA glycosylase (AAG). *Biochemistry*, **48**, 1850–1861.
41. Saparbaev,M., Mani,J.C. and Laval,J. (2000) Interactions of the human, rat, *Saccharomyces cerevisiae* and *Escherichia coli* 3-methyladenine-DNA glycosylases with DNA containing dIMP residues. *Nucleic Acids Res.*, **28**, 1332–1339.
42. Lazzaro,F., Giannattasio,M., Puddu,F., Granata,M., Pellicioli,A., Plevani,P. and Muzi-Falconi,M. (2009) Checkpoint mechanisms at the intersection between DNA damage and repair. *DNA Repair*, **8**, 1055–1067.
43. Athanasiadis,A., Rich,A. and Maas,S. (2004) Widespread A-to-I RNA editing of Alu-containing mRNAs in the human transcriptome. *PLoS Biol.*, **2**, e391.
44. Paul,M.S. and Bass,B.L. (1998) Inosine exists in mRNA at tissue-specific levels and is most abundant in brain mRNA. *EMBO J.*, **17**, 1120–1127.
45. Nishikura,K. (2006) Editor meets silencer: crosstalk between RNA editing and RNA interference. *Nat. Rev. Mol. Cell. Biol.*, **7**, 919–931.
46. Schaub,M. and Keller,W. (2002) RNA editing by adenosine deaminases generates RNA and protein diversity. *Biochimie*, **84**, 791–803.
47. Abolhassani,N., Iyama,T., Tsuchimoto,D., Sakumi,K., Ohno,M., Behmanesh,M. and Nakabeppu,Y. (2010) NUDT16 and ITPA play a dual protective role in maintaining chromosome stability and cell growth by eliminating dIDP/IDP and dITP/ITP from nucleotide pools in mammals. *Nucleic Acids Res.*, doi:10.1093/nar/gkp1250.